

Omni²: Unifying Omnidirectional Image Generation and Editing in an Omni Model

Liu Yang¹, Huiyu Duan¹, Yucheng Zhu¹, Xiaohong Liu¹, Lu Liu¹, Zitong Xu², Guangji Ma²,
Xiongkuo Min¹, Guangtao Zhai¹, Patrick Le Callet³

¹Shanghai Jiao Tong University, Shanghai, China

²University of Electronic Science and Technology of China, Sichuan, China

³Université de Nantes, Nantes, France

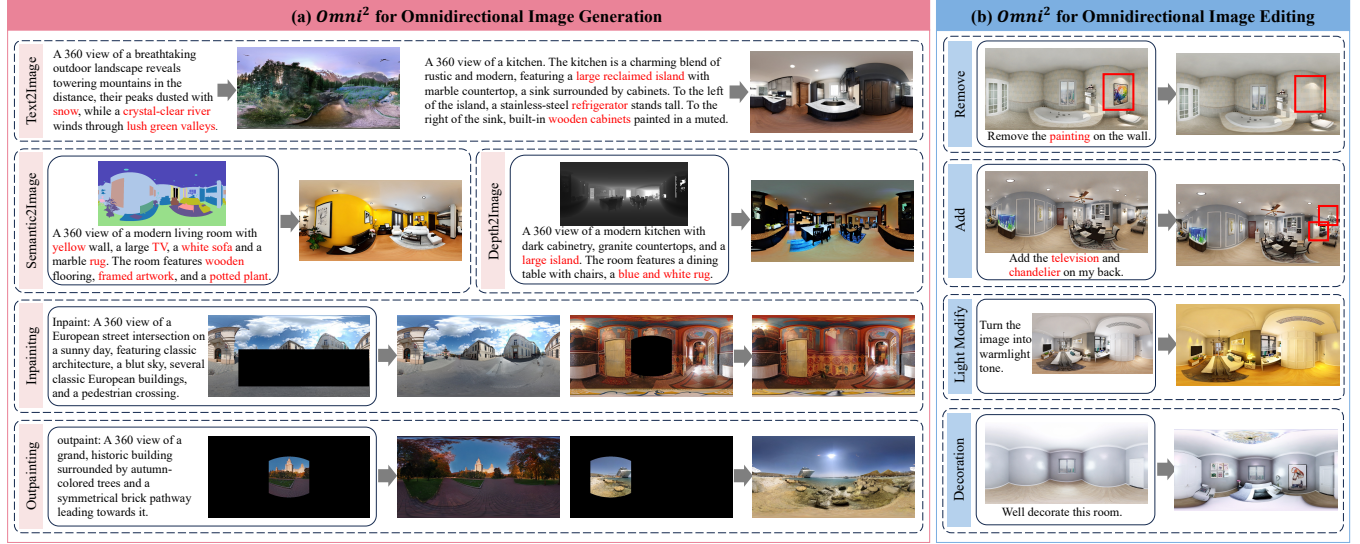


Figure 1: We propose the first omni model for omnidirectional image generation and editing, termed *Omni²*. *Omni²* is capable of handling both omnidirectional image generation and editing with various input conditions, demonstrating strong potential across diverse tasks, as demonstrated in (a) and (b).

Abstract

360° omnidirectional images (ODIs) have gained considerable attention recently, and are widely used in various virtual reality (VR) and augmented reality (AR) applications. However, capturing such images is expensive and requires specialized equipment, making ODI synthesis increasingly important. While common 2D image generation and editing methods are rapidly advancing, these models struggle to deliver satisfactory results when generating or editing ODIs due to the unique format and broad 360° Field-of-View (FoV) of ODIs. To bridge this gap, we construct *Any2Omni*, the first comprehensive ODI generation-editing dataset comprises 60,000+ training data covering diverse input conditions and up to 9 ODI generation and editing tasks. Built upon *Any2Omni*, we propose an *Omni* model for *Omni*-directional image generation and editing (*Omni²*), with the capability of handling various ODI generation and editing tasks under diverse input conditions using one model. Extensive experiments demonstrate the superiority and effectiveness of the proposed *Omni²* model for both the ODI generation and editing tasks.

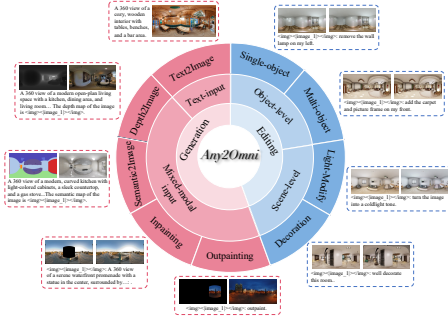
Keywords

Omnidirectional Image Generation, Omnidirectional Image Editing, Generative Models, Virtual Reality

1 Introduction

With the rapid advancement of virtual reality (VR) technology, 360° omnidirectional images (ODIs) have gained increasing attention. However, capturing ODIs requires expensive and specialized hardware, making ODI synthesis a crucial task. While 2D image generation techniques have gradually matured with the rapid advancement of AIGC [7, 24, 30], ODI generation remains underexplored. Previous works, such as MVDiffusion [29], can only generate ODIs with a limited vertical Field-of-View (FoV) of $360^\circ \times 90^\circ$, restricting its applicability in real-world scenarios. Though some other methods [8, 40, 42] are capable of generating full $360^\circ \times 180^\circ$ ODIs, they primarily focus on text-driven ODI generation, while ignoring other input conditions such as narrow viewport images, semantic maps, depth maps, *etc.*

High-quality 2D image editing datasets [5, 26, 43] have recently driven the advancement of image editing models [11, 43]. In the context of ODIs, editing is of great importance for enhancing quality of experience in immersive environment. However, omnidirectional image editing remains unexplored. Unlike 2D images, ODIs are stored in the warped equirectangular projection (ERP) format, thus making common 2D image editing algorithms cannot be directly applied. An alternative approach is applying 2D editing models on the designated single view of an ODI after viewport splitting,



Task Type	Category	Sub-category	Input Condition	# training	# testing
Generation	Text2Image	short-caption	text	10,000	1,000
		detailed-caption	text	10,000	1,000
	Semantic2Image	-	image+text	6,500	500
	Depth2Image	-	image+text	7,000	700
	Outpainting	-	image+text/image	2,938/2,941	500/500
Editing	Object-level Editing	single-object removal/add	image+text	2,946/2,950	500/500
		multi-object removal/add	image+text	6,690	1000
	Scene-level Editing	Light-Modify	image+text	5,889	500
		Decoration	image+text	4,698	500

Table 1: Detailed data distribution in Any2Omni dataset.

but it is both time-consuming and inefficient, and may generate inconsistent views. Moreover, due to the unique depth and spatial characteristics of omnidirectional images, conventional 2D editing models struggle to understand the spatial relationships between viewports or even within individual ODI views, making the split-and-edit approach impractical. Therefore, dedicated ODI editing dataset and method are necessary to advance research in this domain.

Built upon the rapid progress in 2D image generation and editing, integrating these tasks into a unified framework has become increasingly popular [31, 37, 39]. In this paper, we aim to unify ODI generation and editing into an efficient model. To this end, we first introduce *Any2Omni*, the first comprehensive dataset for omnidirectional image generation and editing tasks. As shown in Table 1, our dataset integrates multiple input modalities for ODI generation tasks. For the newly defined omnidirectional image editing tasks, we start by proposing a simple yet effective pipeline capable of generating high-quality, object-level indoor editing samples. Additionally, we introduce two scene-level ODI editing tasks utilizing existing ODI datasets [44]. Overall, our Any2Omni dataset comprises over **60,000** training samples, covering **9** categories of omnidirectional image generation and editing tasks with various input conditions.

Based on Any2Omni, we further introduce the first omni model for omnidirectional image generation and editing, termed *Omni*². *Omni*² adopts a simple yet effective Transformer-based framework to support $360^\circ \times 180^\circ$ high-quality omnidirectional image synthesis under a variety of multimodal input conditions. In contrast to existing diffusion-based ODI generation methods, which incorporate additional attention blocks for multi-view consistency [29, 42], we introduce a novel approach by executing viewport-based bidirectional attention within a unified Transformer. Our model demonstrates superior performance across a wide range of ODI generation and editing tasks with various input conditions, as shown in Fig. 1.

The main highlights of this work include:

- We unify the ODI generation and editing tasks. To the best of our knowledge, our study is the first work to achieve multimodal input-based ODI generation for various tasks, and the first to explore ODI editing.
- We construct *Any2Omni*, the first comprehensive dataset for omnidirectional image generation and editing that contains over 60,000 training samples covering 9 ODI generation and editing tasks with various input conditions.

- We propose *Omni*², the first omni model for omnidirectional image generation and editing. *Omni*² is capable of processing various input conditions and producing high-quality, viewport-consistent ODIs.
- Extensive experimental results demonstrate that the proposed *Omni*² model exhibits state-of-the-art performance on ODI generation tasks, and shows great potential on ODI editing tasks.

2 Related Work

2.1 Omnidirectional Image Generation

Although 2D image generation has made significant progress recently, omnidirectional image generation remains notably limited. Prior works, such as MultiDiffusion [4], employ pretrained diffusion model to generate long images from text input. However, these images are not composed of stitched multi-view images thus are not aligned with the true projection process of ODIs. MVDiffusion [29] solves this problem by synchronously generating eight overlapping views using pretrained stable diffusion model [24] and introduces Correspondence-Aware Attention (CAA) module to ensure viewport consistency. However, it only generates the central perspectives, omitting the top and bottom views, limiting its applicability in real-world scenarios. Other methods like DiffPano [40] and PanFusion [42] are able to generate omnidirectional images with the full FoV, yet they are still limited to specific input conditions, and lack support for generation tasks with other input conditions, such as depth-to-image generation and outpainting, etc.

2.2 Independent Image Generation and Editing

Recent advancements in 2D generative models have been remarkable, with methods such as the Stable Diffusion series [21, 24] and DALL-E [22] demonstrating superior generative capabilities. In addition, the emergence of large-scale, high-quality 2D image editing datasets [5, 26, 41, 43] and benchmarks [34] have significantly advanced image editing models [16, 26, 35]. However, limited works have been proposed for ODI generation as aforementioned, and the field of ODI editing remains unexplored, despite the essential role ODI plays in real-world applications.

2.3 Unified Image Generation and Editing

With the rapid advancement of 2D image generation and editing models, unified 2D generation-editing datasets and models have

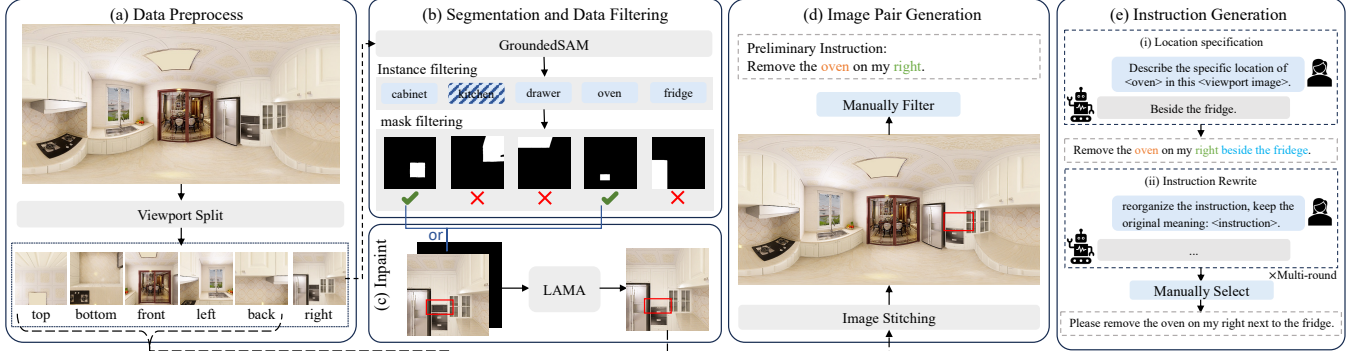


Figure 2: We present a simple yet effective pipeline for constructing high-quality object-level indoor omnidirectional image editing dataset. Our pipeline is mainly consisted of two parts, i.e., image pair generation and instruction refinement. (a) The ODI input undergoes viewport splitting to generate six perspective images. (b) Viewport image is processed through a segmentation model for instance-level segmentation and class labeling, followed by dual-stage filtering for quality control. (c) A selected instance is removed via inpainting [28]. (d) The edited viewport image is seamlessly stitched with other perspective images to form edited ODI. (e) InternVL2-5 [9] is deployed to refine editing instructions, adding positional details and enhancing linguistic diversity.

emerged. Compared to single-task models such as text-to-image (T2I) generation or image inpainting, unified multimodal-input generation and editing models offer broader applications. DreamOmni [37] introduces a synthetic data pipeline for generating large-scale multi-task image generation and editing training examples and constructs a unified image generation and editing model. OmniGen [39] constructs a large-scale, diverse dataset, X2I, encompassing various image generation and editing tasks for joint training, and further proposes a unified diffusion-transformer model OmniGen, which demonstrates strong capabilities across various text-to-image generation and downstream tasks. However, in the field of ODI synthesis, there are still many unexplored tasks, let alone comprehensive datasets and models. To address these issues and to advance research on omnidirectional image synthesis, we introduce Any2Omni, the first comprehensive dataset for ODI generation and editing, and Omni², a unified model that shows strong capabilities across multiple ODI generation and editing tasks.

3 Any2Omni Dataset

To gain the capability of handling various image generation and editing tasks, it is essential to build a comprehensive dataset for model training. Though some omnidirectional image generation works have tried training on captioned existing ODI datasets [6, 10, 32, 38], a truly comprehensive ODI generation dataset remains absent. Furthermore, there’s currently no dataset for omnidirectional image editing. In this section, we introduce *Any2Omni*, the first comprehensive dataset for omnidirectional image generation and editing. For generation subset, we construct a diverse ODI generation dataset to support multiple ODI generation tasks with various input conditions. For ODI editing subset, we start by proposing a simple yet effective pipeline for object-level indoor ODI editing, and further propose a range of insightful indoor ODI editing tasks. Our *Any2Omni* contains over **60,000** training examples with **9** tasks, establishing it as the first large-scale and comprehensive dataset dedicated to advancing research in **ODI generation and editing**.

3.1 Generation Subset

Although prior works have explored T2I and outpainting tasks for ODIs [12, 29, 32, 33, 42], they address these tasks separately, each tailored to a specific input-output format. Besides, we believe there are insightful ODI generation tasks that remain unexplored. To this end, we construct a comprehensive generation subset, encompassing 5 ODI generation tasks: text2ODI, inpainting, outpainting, semantic2ODI, and depth2ODI, among which we newly proposed semantic2ODI and depth2ODI as we believe they present significant opportunities for advancing ODI generation. We collect ODIs from existing datasets, including SUN360 [38], Structured3D [44], etc., and caption these images using InternVL2-5 [9] to generate text condition. For inpainting and outpainting tasks, images are randomly masked as input image conditions. For semantic2ODI and depth2ODI tasks, we use paired images from Structured3D and Pano3D [3], respectively, and generate captions to provide text conditions for these tasks. The detailed construction process is provided in the supplementary materials.

3.2 Editing Subset

While 2D image editing has achieved significant advancement, the field of omnidirectional image editing remains unexplored, primarily due to the scarcity of high-quality training datasets. As object removal and addition are among the most fundamental tasks in image editing, in this work, we begin to address the challenge of constructing ODI editing dataset with a specific focus on the object-level removal and addition tasks. Additionally, we propose two scene-level ODI editing tasks that effectively leverage the existing ODI dataset [44], contributing to the advancement of ODI editing.

3.2.1 Object-level Indoor Editing Pipeline. The primary challenge in generating ODI editing datasets lies in creating editing image pairs where only a partial set of objects is precisely added or removed, while the other details of the image are retained. Due to the rarity of ODIs in social media applications, it is not feasible to directly collect editing image pairs through web crawling, as is

done with 2D editing datasets [11, 27]. Since constructing manually annotated datasets is impractically time-consuming, 2D image editing datasets are often built by either applying 2D generation methods [5] or utilizing existing 2D-related datasets. For instance, Inst-Inpaint [41] leverages existing dataset [17] to obtain scene graphs within the image, which significantly simplifies the task. However, due to the immaturity of current ODI generation methods and limited sources of ODI-related datasets, we are forced to build the omnidirectional image editing dataset from scratch. In response, we develop a pipeline that can generate high-quality editing image pairs and detailed editing instructions from a single, unconditioned indoor ODI input, as illustrated in Fig. 2.

Compared to outdoor omnidirectional images, indoor ODIs are often more diverse and contain easily segmentable objects. As an initial attempt at omnidirectional image editing, we select Structured3D [44], a large-scale indoor ODI dataset, to generate object-level removal/addition image pairs. Inspired by [41], we constructed our editing image pairs through a pipeline that integrates segmentation and inpainting models to generate precise edited image pairs. However, unlike Inst-Inpaint, which relies on object categories provided by the scene graphs in the GQA dataset [17] for instance segmentation, our task requires an algorithm capable of both detecting instances and outputting corresponding instance categories. To accomplish this, we choose GroundedSAM [23] due to its ability to effectively detect and classify instances in a single pass. Directly applying segmentation on the ERP formatted ODIs yields imprecise results. Furthermore, given the richness of objects in indoor scenes, we propose to generate **editing pairs with predefined viewports**. Specifically, we first split the ODIs into six viewpoints: front, back, left, right, top, and bottom. Then, segmentation is applied on each individual viewport, as shown in Fig. 2(a).

We perform dual-stage post-processing after the segmentation process to ensure data quality, as illustrated in Fig. 2(b). First, we apply instance filtering to remove instances that are irrelevant for our object-level editing purpose, such as “floor”, “cityscape”, and “bedroom”. Since the inpainting operation is applied to each individual viewport, instances that span across multiple viewports may experience disruptions in scene consistency when inpainting is applied to each viewport separately. To address this, we implement an automatic instance filtering method, where instances with segmentation masks located at the image edges are discarded. This process effectively filters out approximately 60% of the segmentation results.

With the selected instance classes and corresponding segmentation masks, we adopt LAMA [28] to inpaint the instances, thereby generating object-removal outputs, shown in Fig. 2(c)-(d). The outputs are manually selected to ensure image quality. Inspired by [11, 41], object-addition pairs are generated by swapping the input and output images. By executing multiple rounds of the pipeline on the same perspective image and stitching together images edited from various viewports, we further obtain a set of **multi-object editing image pairs**.

Preliminary editing instructions are formed using the detected instance class and the viewport information in the format as “Remove the <instance class> on my <viewport>.” In certain editing cases, the relative location of the object should be pointed out. To address this, we input both the original image and segmented instance

class into Internvl2-5 [9], instructing it to generate relative position descriptions, as shown in Fig. 2(e). With these relative position descriptions, we create more detailed editing instructions: “Remove the <instance class> on my <viewport> beside the <reference instance>.” For multi-object editing, the instructions are formed as: “Add the <instance class1> beside the <reference instance1> on my my <viewport1> and <instance class2> on my <viewport2>.” To ensure data diversity, we further utilize Internvl2-5 [9] to refine the generated editing instructions, thereby creating a range of diverse expressions that contribute to improving the model’s robustness. The instruction generation process is carried out over multiple iterations, during which we manually select the most appropriate instructions.

3.2.2 Scene-level ODI Editing. The ability to manipulate entire scenes is a defining characteristic that enhances immersion and interactivity in omnidirectional images within virtual reality applications. To this end, we introduce two novel scene-level indoor editing tasks, namely light modify and indoor decoration, designed to enable comprehensive editing of ODIs. We collect the image pairs from Structured3D and standardize the tasks into the input-output pair format, as detailed in the supplementary.

4 Proposed Method

In this section, we introduce our *unified* model, **Omni**², towards unifying omnidirectional image generation and editing from various condition inputs in free form using one model.

4.1 Overall Architecture

The overall Architecture of Omni² is presented in Fig. 3, which adopts a pretrained Transformer as the denoising network. The model takes arbitrarily interleaved text and images in free form as input conditions, which are then tokenized and fed into the Transformer for denoising, along with timestep tokens and viewport noise. The last hidden state is then passed through a feature decoder to obtain the final viewport embeddings. During inference, the viewport embeddings are subsequently fed into a VAE decoder to generate viewport images, which are then stitched together to form a seamless ODI output.

4.2 Model Design

4.2.1 Input Embedding. We propose generating separate viewports instead of treating the entire ODI as a single entity, in order to ensure viewport consistency and align with the capture process of ODIs. To address this, the noise input is defined on a viewport basis for the viewport-based diffusion process, as shown in Fig. 3.

Input image condition is also viewport tokenized to align with the output. Given an ODI as an input image, we employ a viewport tokenizer to convert the image into viewport-based tokens. Specifically, the input ODI is divided into six overlapping viewports, each of which is then transformed into viewport-based latent representations using a frozen VAE encoder. These representations are then flattened into a sequence of visual tokens with the patch size set to 2 following [20]. During training, the viewport noise is formulated as:

$$z_t^i = tz^i + (1 - t)\epsilon^i \quad (1)$$

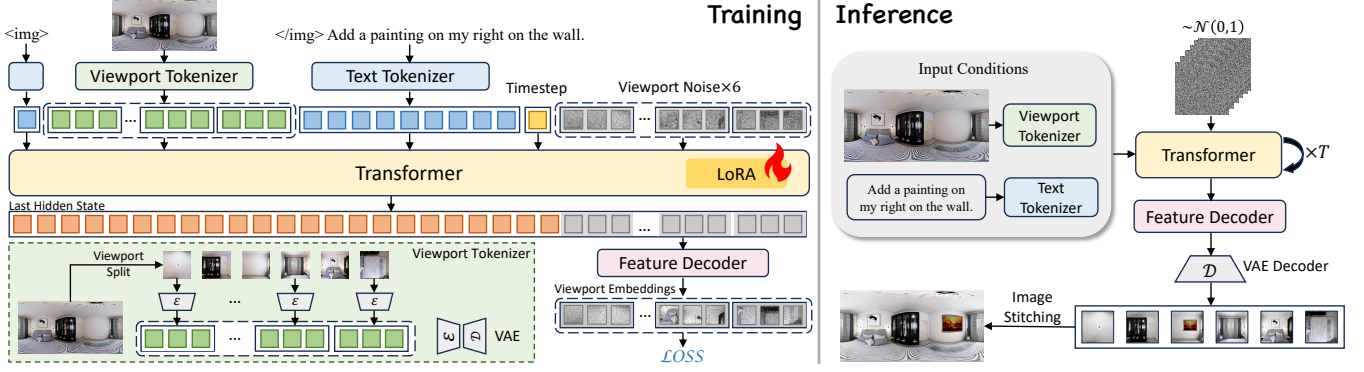


Figure 3: Overview of proposed Omni². Input prompt and Image are tokenized through text tokenizer and viewport tokenizer separately before feeding into a simple yet effective transformer for viewport image generation. During inference, the generated viewports are seamlessly integrated to reconstruct a high-quality omnidirectional image.

where z^i is the viewport-based latent representation of the ground truth $\{x_i\}_{i=1}^6$, t is the diffusion timestep and $\epsilon^i \sim \mathcal{N}(0, I)$ is the Gaussian noise. During the inference stage, each viewport noise is formulated as a random sampled Gaussian noise, as shown in Fig. 3.

The text prompt and timestep are also tokenized and fed into the pretrained transformer to facilitate the denoising process.

4.2.2 Attention Mechanism for Viewport Consistency. In omnidirectional image generation, maintaining viewport consistency is especially crucial. Previous works often adopt diffusion model for ODI generation, with external attention modules designed to ensure viewport consistency [29, 42]. However, these approaches introduce additional training parameters and lack holistic control across viewports, as viewports are generated separately [29]. In contrast, we propose to leverage and modify the attention mechanism within the Transformer architecture itself to achieve multi-view consistency. Specifically, we adopt the Transformer from Phi-3 [1] as the denoising network. We believe that viewports should be treated equally during the generation process to maintain viewport consistency. To this end, we propose a novel approach to apply bidirectional attention mechanism within the viewport sequences while maintain the causal attention mechanism elsewhere. This approach is not only simpler but also effectively preserves viewport consistency. Furthermore, since viewports are generated using the shared model, it allows for greater overall control over the image, ensuring more coherent results across all generated views.

4.2.3 Omnidirectional Image Generation. The final hidden state from the Transformer is passed into a feature decoder to map the language space features into latent representations for each viewport. We utilize the final layer from [20] to accomplish this process. The VAE decoders then decode the generated viewport representations into predicted viewports, which are subsequently stitched together to form a seamless omnidirectional image.

4.3 Training

4.3.1 LoRA-based Finetuning. 2D generation models possess excellent prior knowledge of image generation and strong text comprehension capabilities. Due to the limited scale of omnidirectional

images, we use the VAE from SDXL [21] and initialize the Transformer with pretrained weights from [39] to take advantage of the excellent generation ability on 2D images. During training, only the Transformer is finetuned using LoRA [15] to improve training efficiency and retain generalization capability as much as possible.

4.3.2 Loss Function. Flow matching [19] is employed to train the model. We extend the loss from single-view to multi-view. For each training step, we randomly sample a timestep t for all the viewport images $\{x_i\}_{i=1}^N$. The loss function is defined as:

$$\mathcal{L} = \mathbb{E} \left[\sum_{i=1}^N \|(z^i - \epsilon^i) - v_\theta(z_t^i, t, c)\|^2 \right] \quad (2)$$

where $z^i = \{\mathcal{E}(x_i)\}_{i=1}^N$ represents the latent embeddings of the i -th viewport image, $\epsilon^i \sim \mathcal{N}(0, 1)$ is the Gaussian noise, z_t^i is the noised latent for the i -th viewport as defined in Eq. 1, and c denotes the embed condition.

For tasks like light modify and object-level editing, different regions should be adjusted with varying intensities. Specifically, for light modify, distinct areas require different levels of adjustment, while in object-level editing, only a small portion of the regions needs to be modified, thus we make slight modifications to the loss function for these tasks to enable the model to learn the appropriate intensities and to prevent it from simply copying the input image as the output, as discussed in [39]. This was achieved by introducing a weighted loss, where regions that differ significantly from the input image are assigned higher weights. However, although the decoration task belongs to editing, since the change is made to the overall image, applying weighted loss leads to unsatisfactory results. Therefore, we use the original loss for the decoration task.

5 Experiment

5.1 Implementation Details

5.1.1 Training Settings. We train the Omni² model on our Any2Omni dataset using an **all in one** training strategy, *i.e.*, all nine tasks, including both generation and editing, are trained simultaneously. The image resolution is set to 512×1024 and the viewport FoV is set to 110° with resolution of 256×256 . The total number of training step is 10k. The training is performed using the AdamW optimizer

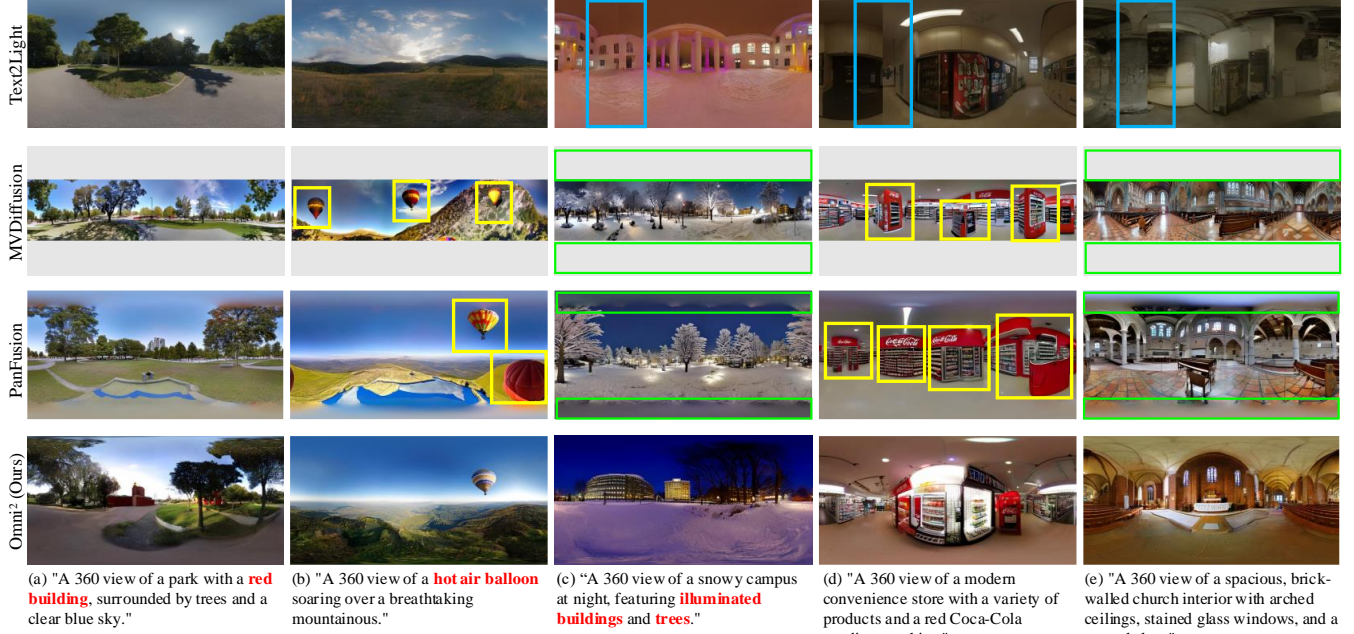


Figure 4: Text to ODI comparison between Text2Light [8], MVDiffusion [29], PanFusion [42] and ours. We highlight the left-right inconsistency, repeating objects in different views and top-bottom blurriness/missing with corresponding color boxes. Objects that are missing in some baselines but present in our method are **bolded and highlighted in red in the prompts.**

Table 2: Comparison with state-of-the-art methods on text to omnidirectional image task. *Since MVDiffusion cannot generate full-FOV ODIs, we evaluate its performance here for reference purposes.

Methods	FID↓	IS↑	CS↑	Inference Time(s)↓
Text2Light [8]	91.05	4.90	0.7007	135.36
MVDiffusion* [29]	92.59	6.64	0.5367	252.08
PanFusion [42]	80.66	7.36	0.8463	67.83
Omni ² (Ours)	47.32	7.62	0.8887	22.55

Table 3: User study of text to ODIs.

Methods	Image Quality↑	Image-Text Consistency↑	Omni-Scene Consistency↑
Text2Light [8]	2.17	2.28	2.78
PanFusion [42]	3.33	3.94	4.44
Omni ² (Ours)	4.06	4.72	4.83

with a batch size of 16 and a learning rate of $1e^{-3}$, utilizing 2 A6000 GPUs.

5.1.2 Inference Settings. The sampling steps T is set to 50. The guidance scale and image guidance scale are adjusted according to the specific tasks. More implementation details are provided in the supplementary material.

5.2 Text to Image

5.2.1 Qualitative Results. We compare the text2ODI performance of proposed Omni² with other 3 models trained on their respective datasets. The qualitative comparison results are presented in Fig. 4. Images generated by MVDiffusion [29] are padded gray in the top and bottom since MVDiffusion can only generate images

with 90° vertical FoV. The images are rotated by 90° to better visualize left-right consistency. As can be observed, ODIs generated by Text2Light [8] exhibit poor left-right consistency and fail to capture detailed object specified in the text prompt, such as the missing “red building” in (a) and the “hot air balloon” in (b). Despite the top-bottom view missing problem, MVDiffusion tends to generate repeating objects across different viewports since the ODIs are stitched from 8 viewports generated by SD [24] blocks, separately, resulting in a loss of overall image coherence. ODIs generated by PanFusion [42] suffer from top-bottom blurriness and also exhibit insensitivity to specific details in the text prompt, *e.g.*, missing illuminated buildings in (c). In contrast, our model is capable of generating ODIs with clear $360^\circ \times 180^\circ$ FoV, while preserving fine details from the text prompt, demonstrating superior text2ODI performance for both indoor and outdoor ODI generation.

5.2.2 Quantitative Results. Table 2 presents the quantitative results of text2ODI task. We use Fréchet Inception Distance (FID) [14], Inception Score (IS) [25] and Clip Score (CS) [13] to compare the quality of ODIs generated by Omni² with that by other methods. We also report inference time on a single A6000 for efficiency comparison. It can be observed that our model outperforms others in terms of all the evaluation metrics. Moreover, our method has a substantial advantage in inference time due to the attention mechanism using kv-cache.

5.2.3 User Study. To better quantize the performance of different methods, we collect 108 text prompts and recruit 20 volunteers to rate the generated ODIs from three perspectives: image quality, image-text consistency and omni-scene consistency. Experimental results presented in Table 3 show that our proposed Omni² exhibits



Figure 5: Outpainting comparison between SIG-SS [12], OmniDreamer [2], PanoDiffusion [36], PanoDiff [32], and ours.

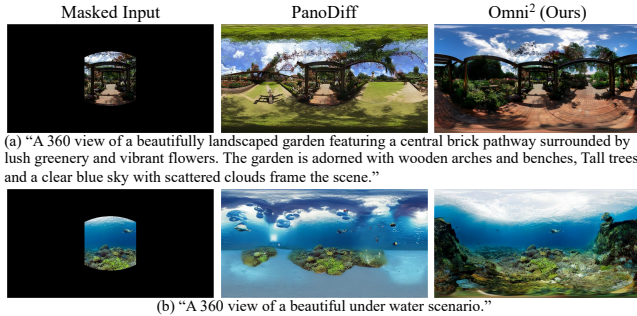


Figure 6: Text-instructed outpainting comparison between PanoDiff [32] and ours.

Table 4: Comparison with state-of-the-art methods on outpainting task.

Task	Image Input		Text-Image Input		
	FID↓	IS↑	FID↓	IS↑	CS↑
SIG-SS [12]	66.67	5.04	N/A	N/A	N/A
OmniDreamer [2]	73.80	5.15	N/A	N/A	N/A
PanoDiffusion [36]	127.30	4.19	N/A	N/A	N/A
PanoDiff [32]	61.03	6.30	45.54	6.78	0.8535
Omni ² (Ours)	44.13	6.86	37.40	6.93	0.8620

an overall superior performance, demonstrating its strong capability of ODI generation.

5.3 Multi-modal to Image

We compare the performance of our model with the state-of-the-art methods on the ODI outpainting task. For image-based outpainting, we report FID and IS scores for comparison. For text-guided outpainting, we add the CS metric to evaluate the correspondence between image and text. The results are presented in Table 4. Our model achieves state-of-the-art performance on ODI outpainting tasks, both with and without text prompts.

The qualitative results of image conditioned outpainting are presented in Fig. 5. We only provide the outpainting results from center viewport here, outpainting results from diverse input masks are presented in the supplementary. It should be noted that since we do not know the specific data split for these models, images in our test set could be in their training set. As can be seen in the figure, outpainting results generated by SIG-SS [12] and OmniDreamer [2] suffer from noticeable boundary inconsistencies, while PanoDiffusion [36] tends to produce images with evident artifacts. Although PanoDiff [32] demonstrates relatively better visual quality in terms of boundary consistency, the outpainting content appears less semantically reasonable. In contrast, our model significantly outperforms these baselines by generating semantically

meaningful and visually coherent images with superior boundary consistency and enhanced overall visual fidelity.

We also compare the performance of proposed Omni² with PanoDiff on text-guided ODI outpainting, qualitative results are shown in Fig. 6. PanoDiff struggles to generate semantically plausible results, e.g., grass in the sky in Fig. 6 (a). In addition, artifacts and meaningless objects appear in the generated ODIs. In contrast, our proposed Omni² is able to generate meaningful content that is consistent with the text prompt.

Due to the limited number of dedicated methods for ODI inpainting, semantic2image, and depth2image, the qualitative results of these tasks are presented in the supplementary material.

5.4 Omnidirectional Image Editing

Since there is no existing ODI editing method, we compare our method with existing 2D image editing methods in two aspects: directly applying existing editing methods on ODI, and editing the designated viewport separately after viewport splitting.

We first compare our method with directly applying 2D editing on ODIs. The results are shown in Fig. 7. As illustrated, HQ-Edit [18] generates images that are completely unrelated to the source image, while InstructPix2Pix [5] fails to understand the instructions and produces incorrect images, such as the wall being mistakenly painted yellow in Fig. 7(b). Although MagicBrush [43] seems to partially understand some of the editing instructions and makes adjustments to the source image, it struggles with understanding the direction of the edits, which is critical for immersive VR editing. Furthermore, all these methods fail to truly understand the object within the image, as can be clearly seen in fig. 7(a), possibly due to the fact that 2D editing models are not trained to understand the warped ERP format.

We also compare our method with applying 2D editing method on designated views. The results for the edited viewport are presented in Fig. 8. We split the view such that the targeted object is centered in the viewport image. As can be observed, both Instruct-Pix2Pix and HQ-Edit fail to comprehend the instructions while MagicBrush introduces noticeable artifacts, as highlighted in the yellow box. Additionally, the added object lacks the level of detail produced by our method. More importantly, this split-and-edit approach is not applicable to real-world scenarios, as it overlooks the global coherence of the entire 360° image and the complex interactions between different regions of the scene.

The experimental results clearly demonstrate the ineffectiveness of applying 2D editing methods on ODIs, which underscores the importance of developing methods tailored to the unique demands of omnidirectional image editing.



Figure 7: Visual comparison of directly applying existing 2D editing methods [5, 18, 43] on ODIs versus our method.

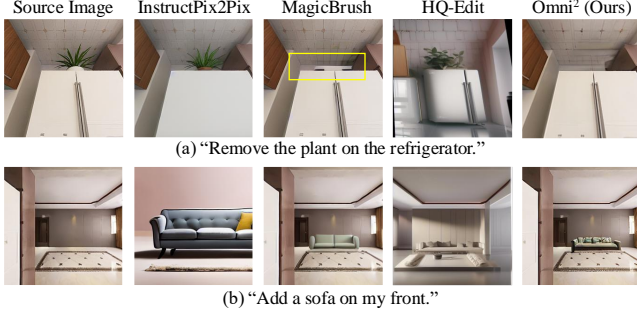


Figure 8: Visual comparison of directly applying existing 2D editing methods [5, 18, 43] on designated views of ODIs versus our method. Only the designated view is presented.

5.5 Ablation Study

In this section, we conduct ablation studies to validate the utility of the core modules in Omni².

5.5.1 Bidirectional Attention Mask. We adopt bidirectional attention mask within the viewport sequence to maintain viewport consistency. Fig. 9-Top shows the text2image result with causal attention mask. As can be seen, great distortion occurs, and there are clear boundaries for overlapping viewports. The result demonstrate the effectiveness of the proposed viewport-based bidirectional attention mask.

5.5.2 Loss Function. We modify the loss function so that the model learns to modify dedicated regions within the input image while keeping other parts unchanged. For the decoration task, we use the origin loss for better results. Ablation studies are conducted to demonstrate the effectiveness of the modified loss function, with results presented in Fig. 9-Middle and -Bottom. For object-level image editing, the model tends to simply copying the input as output without weighted loss. For the decoration task, since modifications are made on the whole image, applying weighted loss leads to heavy distortion in generated image.

5.5.3 LoRA Rank. The LoRA rank r is set to 16 in the paper, we also compare the influence of different rank and report the quantitative results of text2image task in Table 5. As shown in the table, using $r = 16$ generally performs better than using $r = 8$ and $r = 32$, which further validates the effect of LoRA finetuning.

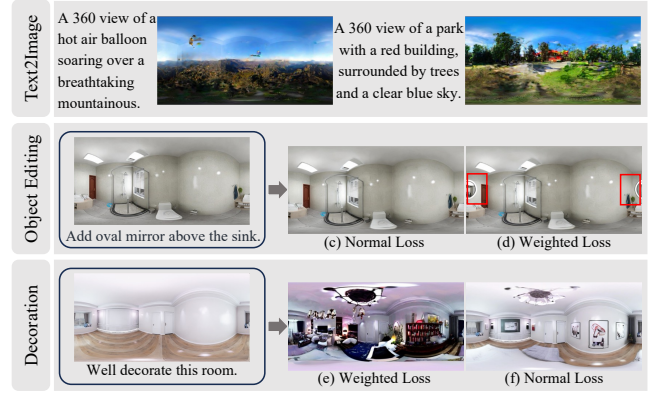


Figure 9: Visual results of ablation studies. Top: ablation on viewport-based bidirectional attention mask; Middle: ablation on weighed loss for object-level editing tasks; Bottom: ablation on normal loss for decoration task.

Table 5: Ablation study on LoRA rank, with T2I performance results reported.

LoRA rank r	FID↓	IS↑	CS↑
8	48.68	6.96	0.8873
32	47.63	7.34	0.8853
16 (Ours)	47.32	7.62	0.8887

6 Conclusion

In this paper, we aim to unify omnidirectional image generation and editing tasks. Specifically, we first construct Any2Omni, the first comprehensive dataset containing 60,000+ data encompassing various ODI generation and editing tasks. Any2Omni contains the first comprehensive multi-task ODI generation subset with diverse input conditions and the first ODI editing subset featuring both object-level and scene-level editing tasks. Based on the dataset, we propose Omni², an omni model for omnidirectional image generation and editing via a Transformer architecture with viewport-based bidirectional attention mechanism, which is able to process multi-modal input conditions and generate high-quality ODIs across various tasks. Extensive experiments demonstrate that our proposed model achieves state-of-the-art performance on various ODI generation tasks and exhibits strong potential for ODI editing tasks.

References

- [1] Marah Abidin, Jyoti Aneja, Hany Awadalla, Ahmed Awadallah, Ammar Ahmad Awan, Nguyen Bach, Amit Bahree, Arash Bakhtiari, Jianmin Bao, Harkirat Behl, et al. 2024. Phi-3 technical report: A highly capable language model locally on your phone. *arXiv preprint arXiv:2404.14219* (2024).
- [2] Naofumi Akimoto, Yui Matsuo, and Yoshimitsu Aoki. 2022. Diverse Plausible 360-Degree Image Outpainting for Efficient 3DCG Background Creation. In *Proceedings of the IEEE/CVF Conference on Computer Vision and Pattern Recognition (CVPR)*. 11441–11450.
- [3] Georgios Albanis, Nikolaos Zioulis, Petros Drakoulis, Vasileios Gkitsas, Vladimiro Sterzentsenko, Federico Alvarez, Dimitrios Zarpalas, and Petros Daras. 2021. Pano3d: A holistic benchmark and a solid baseline for 360deg depth estimation. In *Proceedings of the IEEE/CVF Conference on Computer Vision and Pattern Recognition (CVPR)*. 3727–3737.
- [4] Omer Bar-Tal, Lior Yariv, Yaron Lipman, and Tali Dekel. [n. d.]. Multidiffusion: Fusing diffusion paths for controlled image generation. ([n. d.]).
- [5] Tim Brooks, Aleksander Holynski, and Alexei A Efros. 2023. Instructpix2pix: Learning to follow image editing instructions. In *Proceedings of the IEEE/CVF Conference on Computer Vision and Pattern Recognition (CVPR)*. 18392–18402.
- [6] Angel Chang, Angela Dai, Thomas Funkhouser, Maciej Halber, Matthias Niessner, Manolis Savva, Shuran Song, Andy Zeng, and Yinda Zhang. 2017. Matterport3d: Learning from rgb-d data in indoor environments. *arXiv preprint arXiv:1709.06158* (2017).
- [7] Huiwen Chang, Han Zhang, Jarred Barber, AJ Maschinot, Jose Lezama, Lu Jiang, Ming-Hsuan Yang, Kevin Murphy, William T Freeman, Michael Rubinstein, et al. 2023. Muse: Text-to-image generation via masked generative transformers. *arXiv preprint arXiv:2301.00704* (2023).
- [8] Zhaoxi Chen, Guangcong Wang, and Ziwei Liu. 2022. Text2light: Zero-shot text-driven hdr panorama generation. *ACM Transactions on Graphics (TOG)* 41, 6 (2022), 1–16.
- [9] Zhe Chen, Jiannan Wu, Wenhao Wang, Weijie Su, Guo Chen, Sen Xing, Muyan Zhong, Qinglong Zhang, Xizhou Zhu, Lewei Lu, et al. 2024. Internvl: Scaling up vision foundation models and aligning for generic visual-linguistic tasks. In *Proceedings of the IEEE/CVF Conference on Computer Vision and Pattern Recognition (CVPR)*. 24185–24198.
- [10] Marc-André Gardner, Kalyan Sunkavalli, Ersin Yumer, Xiaohui Shen, Emiliano Gambaletto, Christian Gagné, and Jean-François Lalonde. 2017. Learning to Predict Indoor Illumination from a Single Image. *ACM Transactions on Graphics (SIGGRAPH Asia)* 9, 4 (2017).
- [11] Zigang Geng, Binxin Yang, Tiankai Hang, Chen Li, Shuyang Gu, Ting Zhang, Jianmin Bao, Zheng Zhang, Houqiang Li, Han Hu, et al. 2024. Instructdiffusion: A generalist modeling interface for vision tasks. In *Proceedings of the IEEE/CVF Conference on Computer Vision and Pattern Recognition (CVPR)*. 12709–12720.
- [12] Takayuki Hara, Yusuke Mukuta, and Tatsuya Harada. 2023. Spherical Image Generation From a Few Normal-Field-of-View Images by Considering Scene Symmetry. *IEEE Transactions on Pattern Analysis & Machine Intelligence (TPAMI)* 45, 05 (May 2023), 6339–6353. doi:10.1109/TPAMI.2022.3215933
- [13] Jack Hessel, Ari Holtzman, Maxwell Forbes, Ronan Le Bras, and Yejin Choi. 2021. Clipscore: A reference-free evaluation metric for image captioning. *arXiv preprint arXiv:2104.08718* (2021).
- [14] Martin Heusel, Hubert Ramsauer, Thomas Unterthiner, Bernhard Nessler, and Sepp Hochreiter. 2017. Gans trained by a two time-scale update rule converge to a local nash equilibrium. *Advances in Neural Information Processing Systems (NIPS)* 30 (2017).
- [15] Edward J Hu, Yelong Shen, Phillip Wallis, Zeyuan Allen-Zhu, Yuanzhi Li, Shean Wang, Lu Wang, Weizhu Chen, et al. 2022. Lora: Low-rank adaptation of large language models. *Proceedings of The International Conference on Learning Representations (ICLR)* 1, 2 (2022), 3.
- [16] Yuzhou Huang, Liangbin Xie, Xintao Wang, Ziyang Yuan, Xiaodong Cun, Yixiao Ge, Jiantao Zhou, Chao Dong, Rui Huang, Ruimao Zhang, et al. 2024. Smartedit: Exploring complex instruction-based image editing with multimodal large language models. In *Proceedings of the IEEE/CVF Conference on Computer Vision and Pattern Recognition (CVPR)*. 8362–8371.
- [17] Drew A Hudson and Christopher D Manning. 2019. Gqa: A new dataset for real-world visual reasoning and compositional question answering. In *Proceedings of the IEEE/CVF Conference on Computer Vision and Pattern Recognition (CVPR)*. 6700–6709.
- [18] Mude Hui, Siwei Yang, Bingchen Zhao, Yichun Shi, Heng Wang, Peng Wang, Yuyin Zhou, and Cihang Xie. 2024. Hq-edit: A high-quality dataset for instruction-based image editing. *arXiv preprint arXiv:2404.09990* (2024).
- [19] Xingchao Liu, Chengyue Gong, and Qiang Liu. 2022. Flow straight and fast: Learning to generate and transfer data with rectified flow. *arXiv preprint arXiv:2209.03003* (2022).
- [20] William Peebles and Saining Xie. 2023. Scalable diffusion models with transformers. In *Proceedings of the IEEE/CVF International Conference on Computer Vision (ICCV)*. 4195–4205.
- [21] Dustin Podell, Zion English, Kyle Lacey, Andreas Blattmann, Tim Dockhorn, Jonas Müller, Joe Penna, and Robin Rombach. 2023. Sdxl: Improving latent diffusion models for high-resolution image synthesis. *arXiv preprint arXiv:2307.01952* (2023).
- [22] Aditya Ramesh, Prafulla Dhariwal, Alex Nichol, Casey Chu, and Mark Chen. 2022. Hierarchical text-conditional image generation with clip latents. *arXiv preprint arXiv:2204.06125* 1, 2 (2022), 3.
- [23] Tianhe Ren, Shilong Liu, Ailing Zeng, Jing Lin, Kunchang Li, He Cao, Jiayu Chen, Xinyu Huang, Yukang Chen, Feng Yan, et al. 2024. Grounded sam: Assembling open-world models for diverse visual tasks. *arXiv preprint arXiv:2401.14159* (2024).
- [24] Robin Rombach, Andreas Blattmann, Dominik Lorenz, Patrick Esser, and Björn Ommer. 2022. High-resolution image synthesis with latent diffusion models. In *Proceedings of the IEEE/CVF Conference on Computer Vision and Pattern Recognition (CVPR)*. 10684–10695.
- [25] Tim Salimans, Ian Goodfellow, Wojciech Zaremba, Vicki Cheung, Alec Radford, and Xi Chen. 2016. Improved techniques for training gans. *Advances in Neural Information Processing Systems (NIPS)* 29 (2016).
- [26] Shelly Sheynin, Adam Polyak, Uriel Singer, Yuval Kirstain, Amit Zohar, Oron Ashual, Devi Parikh, and Yaniv Taigman. 2024. Emu edit: Precise image editing via recognition and generation tasks. In *Proceedings of the IEEE/CVF Conference on Computer Vision and Pattern Recognition (CVPR)*. 8871–8879.
- [27] Peter Sushko, Ayana Bharadwaj, Zhi Yang Lim, Vasily Ilin, Ben Caffee, Dongping Chen, Mohammadreza Salehi, Cheng-Yu Hsieh, and Ranjay Krishna. 2025. REALEDIT: Reddit Edits As a Large-scale Empirical Dataset for Image Transformations. *arXiv preprint arXiv:2502.03629* (2025).
- [28] Roman Suvorov, Elizaveta Logacheva, Anton Mashikhin, Anastasia Remizova, Arsenii Ashukha, Aleksei Silvestrov, Naejin Kong, Harshith Goka, Kiwoong Park, and Victor Lempitsky. 2022. Resolution-robust large mask inpainting with fourier convolutions. In *Proceedings of the IEEE/CVF Winter Conference on Applications of Computer Vision (WACV)*. 2149–2159.
- [29] Shitao Tang, Fuyang Zhang, Jiacheng Chen, Peng Wang, and Yasutaka Furukawa. 2023. MVDiffusion: Enabling Holistic Multi-view Image Generation with Correspondence-Aware Diffusion. *arXiv:2307.01097 [cs.CV]* <https://arxiv.org/abs/2307.01097>
- [30] Keyu Tian, Yi Jiang, Zehuan Yuan, Bingyue Peng, and Liwei Wang. 2024. Visual autoregressive modeling: Scalable image generation via next-scale prediction. *Advances in Neural Information Processing Systems (NIPS)* 37 (2024), 84839–84865.
- [31] Xueyun Tian, Wei Li, Bingbing Xu, Yige Yuan, Yuanzhuo Wang, and Huawei Shen. 2025. Mige: A unified framework for multimodal instruction-based image generation and editing. *arXiv preprint arXiv:2502.21291* (2025).
- [32] Jionghao Wang, Ziyu Chen, Jun Ling, Rong Xie, and Li Song. 2023. 360-Degree Panorama Generation from Few Unregistered NFOV Images. In *Proceedings of the 31st ACM International Conference on Multimedia (ACM MM)*. ACM, 6811–6821. doi:10.1145/3581783.3612508
- [33] Qian Wang, Weiqi Li, Chong Mou, Xinhua Cheng, and Jian Zhang. 2024. 360dvd: Controllable panorama video generation with 360-degree video diffusion model. In *Proceedings of the IEEE/CVF Conference on Computer Vision and Pattern Recognition (CVPR)*. 6913–6923.
- [34] Su Wang, Chitwan Saharia, Ceslee Montgomery, Jordi Pont-Tuset, Shai Noy, Stefano Pellegrini, Yasumasa Onoe, Sarah Laszlo, David J Fleet, Radu Soricut, et al. 2023. Imagen editor and editbench: Advancing and evaluating text-guided image inpainting. In *Proceedings of the IEEE/CVF Conference on Computer Vision and Pattern Recognition (CVPR)*. 18359–18369.
- [35] Cong Wei, Zheyang Xiong, Weiming Ren, Xeron Du, Ge Zhang, and Wenhao Chen. 2024. OmniEdit: Building Image Editing Generalist Models Through Specialist Supervision. In *Proceedings of The Thirtieth International Conference on Learning Representations (ICLR)*.
- [36] Tianhao Wu, Chuanxia Zheng, and Tat-Jen Cham. 2024. PanoDiffusion: 360-degree Panorama Outpainting via Diffusion. *arXiv:2307.03177 [cs.CV]* <https://arxiv.org/abs/2307.03177>
- [37] Bin Xia, Yuechen Zhang, Jingyao Li, Chengyao Wang, Yitong Wang, Xinglong Wu, Bei Yu, and Jiaya Jia. 2024. DreamOmni: Unified Image Generation and Editing. *arXiv preprint arXiv:2412.17098* (2024).
- [38] Jianxiong Xiao, Krista A Ehinger, Aude Oliva, and Antonio Torralba. 2012. Recognizing scene viewpoint using panoramic place representation. In *2012 IEEE conference on Computer Vision and Pattern Recognition (CVPR)*. IEEE, 2695–2702.
- [39] Shitao Xiao, Yuezhe Wang, Junjie Zhou, Huaying Yuan, Xingrun Xing, Ruiran Yan, Chaofan Li, Shutong Wang, Tiejun Huang, and Zheng Liu. 2024. Omnigen: Unified image generation. *arXiv preprint arXiv:2409.11340* (2024).
- [40] Weicai Ye, Chenhao Ji, Zheng Chen, Junyao Gao, Xiaoshui Huang, Song-Hai Zhang, Wanli Ouyang, Tong He, Cairong Zhao, and Guofeng Zhang. 2024. Diff-Pano: Scalable and Consistent Text-to-Panorama Generation with Spherical Epipolar-Aware Diffusion. *arXiv preprint arXiv:2410.24203* (2024).
- [41] Ahmet Burak Yildirim, Vedat Baday, Erkut Erdem, Aykut Erdem, and Aysegül Dundar. 2023. Inst-inpaint: Instructing to remove objects with diffusion models. *arXiv preprint arXiv:2304.03246* (2023).

- [42] Cheng Zhang, Qianyi Wu, Camilo Cruz Gambardella, Xiaoshui Huang, Dinh Phung, Wanli Ouyang, and Jianfei Cai. 2024. Taming stable diffusion for text to 360 panorama image generation. In *Proceedings of the IEEE/CVF Conference on Computer Vision and Pattern Recognition (CVPR)*. 6347–6357.
- [43] Kai Zhang, Lingbo Mo, Wenhui Chen, Huan Sun, and Yu Su. 2023. Magicbrush: A manually annotated dataset for instruction-guided image editing. *Advances in Neural Information Processing Systems (NIPS)* 36 (2023), 31428–31449.
- [44] Jia Zheng, Junfei Zhang, Jing Li, Rui Tang, Shenghua Gao, and Zihan Zhou. 2020. Structured3d: A large photo-realistic dataset for structured 3d modeling. In *Proceedings of the European Conference on Computer Vision (ECCV)*. Springer, 519–535.